Binary Fission Studies of Helium-Ion-Induced Fission of Bi^{209}, Ra^{226}, and U^{238}†

J. P. UNIK AND J. R. HUIZENGA
Argonne National Laboratory, Argonne, Illinois
(Received 26 November 1963)

The kinetic energies of coincident fission fragments were measured for helium-ion-induced fission of Bi^{209}, Ra^{226}, and U^{238} with gold-surface barrier detectors and an Argonne three-parameter analyzer. The data obtained at each bombarding energy were analyzed to give total kinetic-energy and mass-yield distributions for fixed values of the average total kinetic energy, and total kinetic-energy distributions as a function of heavy fragment mass M_H. The mass yield distributions for Bi^{209}, U^{238}, and Ra^{226} are single, double, and triple humped, respectively. The total kinetic-energy release for Bi^{209} fission decreases smoothly with increasing values of M_H and its variance remains constant. The total kinetic energy as a function of M_H for all the bombardments of Ra^{226} and U^{238} show structure with a maximum value at $M_H=135$, while each bombardment gives a maximum in the variance of the total kinetic energy at $M_H=131$. This structure in the kinetic energy for Ra^{226} and U^{238} is interpreted in terms of shell structure in the heavy fragment. The larger kinetic energy observed for symmetric fission of heavy elements with energetic particles over that observed for thermal neutron fission is assumed to be due to a smaller effective separation of charge centers at the scission configuration. This effect may possibly result from a temperature-dependent viscosity and tensile strength of the nuclear fluid and leads to the interesting speculation that information on these parameters may be inferred from nuclear fission data. The full width at half-maximum height in the total kinetic-energy distribution for 42-MeV helium-ion-induced fission of Bi^{209} is 16 ± 1 MeV (corrected for neutron emission and experimental dispersion) in excellent agreement with a theoretical calculation of Swiatecki and Nix.

I. INTRODUCTION

THE total kinetic-energy behavior and fission yields for various mass divisions from spontaneous fission of Cf^{252} and thermal-neutron-induced fission of U^{233}, U^{235}, and Pu^{239} have recently been reported by Milton and Fraser.[1] Whetstone[2] has done a comparable study on spontaneous fission of Cf^{252}. Both of these groups utilize a time-of-flight technique for measuring fission-fragment energies. Gibson *et al.*[3] have made similar measurements for thermal-neutron-induced fission of U^{233}, U^{235}, and Pu^{239} with very thin targets placed between two semiconductor particle detectors. All of the above groups of experimenters observed a marked decrease in the total kinetic energy as symmetrical fission is approached. The magnitude of the drop in total kinetic energy for the thermal-neutron-induced fission was approximately 25 to 40 MeV (i.e., the difference between the maximum total kinetic energy which occurs for U^{235}, for example, at $M_1/M_2=1.25$ and the total kinetic energy at symmetry where $M_1/M_2=1$). The semiconductor measurements[3] give a smaller reduction in the kinetic energy for symmetrical fission than do the time-of-flight measurements.[1] This discrepancy is probably associated with experimental difficulties in one or both of the techniques. However, the large deficit in kinetic energy for symmetric fission of U^{233}, U^{235}, and Pu^{239} is well established even though some uncertainty exists for the precise magnitude of the effect. Fission-fragment range measurements[4] which have the advantage of precise mass resolution give a kinetic-energy deficit nearer the solid-state detector results. The time-of-flight technique has also been employed to study helium-ion-induced fission[5] of Th^{232} and U^{233}. For bombarding energies of 21.6–29.1 MeV, this type of fission gave a dip in the average total kinetic energy at symmetry of 9–12 MeV for Th^{232} and 6–8 MeV for U^{233}. The reduction in kinetic energy for symmetrical fission of heavy nuclei has also been observed for photofission,[6] 14-MeV neutron-induced fission,[7] and 23-MeV deuteron-induced[4] fission.

In an effort to examine systematically the kinetic-energy behavior of target nuclei over a wide range in A, we have studied helium-ion-induced fission of Bi^{209}, Ra^{226}, and U^{238} at different bombarding energies with gold surface barrier semiconductor detectors and report the results of these investigations in this paper. Midway through these experiments it was learned that similar experiments were being carried out by Britt, Wegner, and Gursky.[8] These authors studied helium-ion-induced fission of Au^{197}, Bi^{209}, Ra^{226}, and U^{233}, deuteron-induced fission of Ra^{226} and proton-induced fission of Th^{232}. For all the targets except Au^{197} and Bi^{209} they observed a drop in the average total kinetic energy at symmetry. However, for helium-ion-induced fission of Au^{197} and

† Based on work performed under the auspices of the U. S. Atomic Energy Commission.

[1] J. C. D. Milton and J. S. Fraser, Phys. Rev. Letters **7**, 67 (1961); Can. J. Phys. **40**, 1626 (1962).

[2] S. L. Whetstone, Jr., Phys. Rev. **131**, 1232 (1963).

[3] W. M. Gibson, T. D. Thomas, and G. L. Miller, Phys. Rev. Letters **7**, 65 (1961); only results for the thermal neutron fission of U^{235} are included in the above reference. The data on U^{233} and Pu^{239} were reported by W. M. Gibson, Bull. Am. Phys. Soc. **7**, 37 (1962).

[4] J. M. Alexander, M. F. Gazdik, A. R. Trips, and S. Wasif, Phys. Rev. **129**, 2659 (1963).

[5] S. L. Whetstone, Jr., and R. B. Leachman, Bull. Am. Phys. Soc. **6**, 376 (1961).

[6] B. A. Bochagov, A. P. Komar, and G. E. Solyakin, Zh. Eksperim. i Teor. Fiz. **38**, 1374 (1960); **43**, 1611 (1962) [English transls.: Soviet Phys.—JETP **11**, 990 (1960); **16**, 1135 (1963)].

[7] A. N. Protopopov, I. A. Baranov, Yu. A. Selitskii, and V. P. Eismont, Zh. Eksperim. i Teor. Fiz. **36**, 1932 (1959) [English transl.: Soviet Phys.—JETP **9**, 1374 (1959)].

[8] H. C. Britt, H. E. Wegner, and J. C. Gursky, Phys. Rev. Letters **8**, 98 (1962); Phys. Rev. **129**, 2239 (1963).

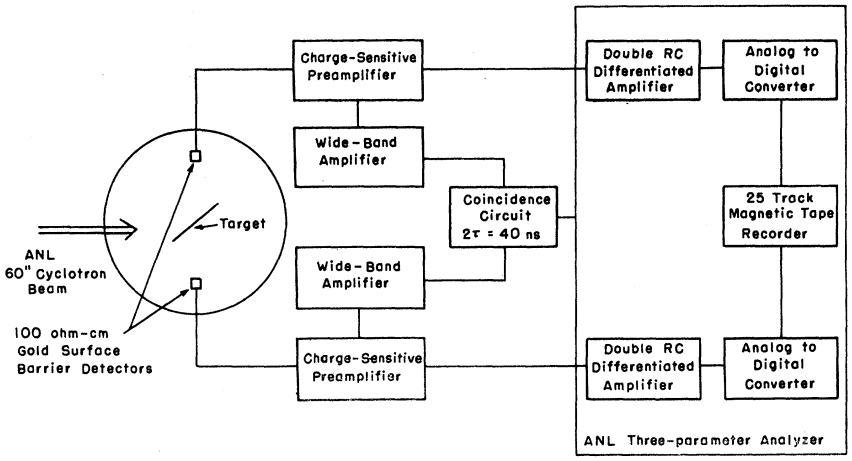

FIG. 1. Schematic diagram of recording system.

Bi^{209} the average total kinetic energy increased continually as the mass ratio approached symmetry.

The present experiments report a study of the kinetic-energy behavior for fissioning systems of widely different mass and varying initial excitation energies. For each bombarding energy of each target the singles and total kinetic energy were determined as a function of primary fission fragment mass as well as for all masses. In addition, the variance of each total kinetic-energy distribution was determined. From the kinetic-energy data, fission-fragment mass yields were computed, including mass yield curves for particular values of the total kinetic energy.

II. EXPERIMENTAL

A. Instrumentation

A schematic diagram of the data recording system is shown in Fig. 1. Fissioning nuclei were produced by bombardment of various targets with the alpha-particle beam of the Argonne 60-in. cyclotron. The cyclotron beam was collimated in this work to a $\frac{1}{16}$-in.-diam cross section and beam currents from 0.02 to 0.1 μA were used. Fission fragments emerging from the thin targets were detected using two 100 Ω-cm gold-surface barrier detectors[9] having collimated 6-mm-diam counting areas. The bias on the detectors was maintained above 15 V to ensure complete collection of the charge produced in the detectors by fission fragments but less than 30 V to minimize the energy loss of beam-scattered alpha particles in the depletion layer. The detectors were fixed at 3 to 4 cm from the target and were initially placed at calculated laboratory angles corresponding to 90 and 270° in the center of mass, assuming full momentum transfer. The angle of one detector was then varied in $\sim$1° increments to maximize the coincidence counting rate. Optimum angles determined in this manner were always within 2° of the calculated angles.

The charge produced by fission fragments in the solid-state detectors was integrated using charge-sensitive preamplifiers. The outputs of the two preamplifiers were then passed into an Argonne three-parameter analyzer.[10] With this analyzer each of the fission-fragment pulse-height distributions was encoded using separate analog-to-digital converters for each detector as eight binary bits (256 channels). Each coincident event was then recorded as two eight-bit numbers in parallel form on a 25-track magnetic tape. The pulse-height analysis and storage were controlled by a coincidence gate. For the bombardment of U^{238} and Bi^{209} a coincidence resolving time of 1 μsec was used. The chance coincidence counting rates in these experiments were measured to be negligible by rotating one detector 15° relative to the other. Because of the narrow 180° center-of-mass angular correlation of the fission fragments, the true coincidences were eliminated in this manner and the chance rates could be measured directly. The Ra^{226} bombardments were performed using a coincidence resolving time of 40 nsec and the chance rates were again negligible.

The coincidence events recorded on magnetic tape were initially sorted using an off-line tape search station[10] to provide the 256 by 256 channel fission-fragment coincident kinetic-energy matrices and the total kinetic-energy distributions. The coincident kinetic-energy matrices were then passed into a computer for final data processing to obtain the fission-fragment mass correlations.

During this work it was found necessary to work at reduced cyclotron beam currents of less than 0.1 μA for increased stability and resolution of the solid-state detectors. At these beam currents the electronic resolution of the counting system measured with a pulse generator was 0.5%. During the course of a bombardment lasting several hours the voltage across the detector would decrease slightly due to radiation damage causing small gain shifts of the order of a few percent. These small gain shifts were corrected by

[9] N. J. Hansen, I. R. E. Trans. Nucl. Sci. **NS-9**, No. 3, 217 (1962).

[10] C. Rockwood and M. Strauss, Rev. Sci. Instr. **32**, 1211 (1961).

previously calibrating the gain of the system as a function of detector voltage, monitoring the voltage during irradiation and periodically making small increases of the amplifier gains to compensate for the decreased detector voltage. In this manner the gain of each system was maintained constant and equal to within 0.5% during the entire course of each irradiation.

Before accumulation of the coincidence data, corrections for the energy loss of the fission fragments traversing the target backing were achieved by suitable parameter adjustments of the recording analyzer. The gains of both systems were adjusted to be identical and then the zero intercept of the analog-to-digital converter for the degraded fragments was increased to compensate for the energy loss. In other cases, the amplifier gain was increased slightly to compensate for the energy loss. After such compensations the spectra of the fragments traversing the target backing and not traversing the backing agreed identically within experimental error thus insuring before a long period of data collection that the energy resolution and pulse-height response of both detectors were identical.

B. Targets

The Bi^{209} metallic target used in this work had an areal density of 50 $\mu g/cm^2$ and was prepared by vacuum volatilization of bismuth metal onto a 100-$\mu g/cm^2$ Al_2O_3 film. A U^{238} target (totally depleted U^{238}) was prepared on a 100-$\mu g/cm^2$ Al_2O_3 foil by diffusion of uranium oxide from a high-temperature diffusion furnace. The areal density of the uranium in this target was 99 $\mu g/cm^2$. The target of Ra^{226} on 100-$\mu g/cm^2$ Ni foil had an areal density of 13 $\mu g/cm^2$ of Ra^{226} and was prepared by vacuum volatilization of $RaCl_3$. The areal densities of the Ra^{226} and U^{238} targets were determined from the measured alpha-particle activities and the known areas of the activities. The areal density of the Bi^{209} target was determined by measuring the relative fission rates of the Bi^{209} target and a known areal density U^{238} target when bombarded with 42-MeV alpha particles. In making this comparison, the fission cross sections and angular distributions measured by Huizenga *et al.* were used.[11,12] Corrections for the energy loss of fragments in the target materials were performed using the data of Alexander and Gazdik.[13]

C. Energy Calibration

For a binary fission event the masses of both fragments can be calculated using the conservation of linear momentum if the initial fragment kinetic energies (before neutron emission) have been measured. Unfortunately, at this time a precise determination of the initial fragment kinetic energies cannot be directly made using solid-state detectors. The fission-fragment pulse heights obtained are not directly proportional to the initial kinetic energies due to (1) the energy loss of fragments traversing the thin "windows" of the detectors, (2) the fission-fragment pulse-height defects inherent in these detectors,[14] and (3) the loss and dispersion in the kinetic energies due to neutron emission from the moving fragments.[15]

The energy loss of the fragments passing through the gold layer plus any effective dead layer present ($\sim$4 MeV) can be measured experimentally only for the most probable or average light and heavy mass fragments. The fission-fragment pulse-height defects for these detectors ($\sim$6 MeV) are not completely understood at this time and hence cannot be accurately measured. In addition to depending on the type of surface-barrier detector used, the pulse-height defect may also depend on the fission-fragment masses.[16]

The effects due to neutrons emitted from the moving fragments are important and should also be considered. The average kinetic-energy loss due to neutron emission ΔE of a fragment of initial mass M_f and energy E_f emitting ν neutrons with masses M_n and with average center-of-mass energies $\bar{E}_n$ is given approximately by Eq. (1).

$$\Delta E \cong \nu M_n \left[\frac{E_f}{M_f} - \frac{\bar{E}_n}{(M_f - M_n)} \right]. \tag{1}$$

The energy loss due to neutron emission cannot be calculated accurately since there is no direct information available on the number of neutrons emitted for a given mass fission fragment at the high-excitation energies used in this work. Information on the number of neutrons emitted for a given mass fission fragment is available only for the spontaneous fission of Cf^{252} (Ref. 17) and thermal neutron fission of U^{233} and U^{235} (Refs. 18 and 19).

In light of the uncertainties in these corrections required to obtain the initial fragment kinetic energies, we have chosen a more direct method to obtain an approximate initial fragment kinetic-energy calibration. The energies of the most probable light and heavy fragments after neutron emission for the spontaneous fission of Cf^{252} can be measured with the surface-barrier detectors using an energy calibration obtained with several well-known alpha-particle groups and a precision pulse generator. The pulse generator is used to normalize the different amplifier gains required to dis-

[11] J. R. Huizenga, R. Chaudhry, and R. Vandenbosch, Phys. Rev. **126**, 210 (1962).
[12] J. R. Huizenga, R. Vandenbosch, and H. Warhanek, Phys. Rev. **124**, 1964 (1961).
[13] J. M. Alexander and M. F. Gazdik, Phys. Rev. **120**, 874 (1960).
[14] H. C. Britt and H. E. Wegner, Rev. Sci. Instr. **34**, 274 (1963).
[15] J. Terrell, Phys. Rev. **127**, 880 (1962).
[16] F. J. Walter, C. D. Moak, J. H. Neiler, H. W. Schmitt, W. M. Gibson, and T. D. Thomas, Bull. Am. Phys. Soc. **8**, 39 (1963).
[17] H. R. Bowman, J. C. D. Milton, S. G. Thompson, and W. J. Swiatecki, Phys. Rev. **129**, 2133 (1963).
[18] J. C. D. Milton and J. S. Fraser, Bull. Am. Phys. Soc. **8**, 370 (1963).
[19] V. F. Apalin, Yu. P. Dobrynin, V. P. Zakharova, I. E. Kutikov, and L. A. Mikaelyan, At. Energy **8**, 15 (1960) [English transl.: Soviet J. At. Energy **8**, 10 (1961)].

play the alpha-particle and fission-fragment spectra. The differences between the values measured in this manner and the initial fragment kinetic energies measured by Milton and Fraser[20] using time-of-flight methods are the sum of the energy loss of the fragments due to neutron emission, the energy loss in the detector window and the pulse-height defect. Values obtained for one detector used in this work are 9.3 ± 1 and 11.0 ± 1 MeV for the most probable light and heavy fragments, respectively. Similar values obtained for another detector used in this work are 11.2 ± 1 and 11.9 ± 1 MeV for the light and heavy fragment, respectively. The combination of these three effects, therefore, displaces the kinetic energies of the most probable light and heavy fragments of Cf^{252} an equal amount within experimental error. Using this fact, the assumption is made that the kinetic energies of all the fragments are displaced equally by these effects and that the kinetic-energy dispersions are small. The first assumption is reasonable since for fission fragments occurring in mass yields greater than 0.5% the calculated energy loss in the gold window (which is a small correction of the order of 4 MeV) does not vary by more than 10%. The calculated energy loss due to neutron emission varies by rather small amounts compared to the total kinetic energies, from 0.3 to 3.3 MeV for the light fragments and from 0.6 to 1.3 MeV for the heavy fragments.[17] If these assumptions are correct, the kinetic energies obtained with the surface-barrier detectors should be displaced to lower kinetic energies approximately an equal amount for all fragments. Since this effect would lead to a displacement of the final kinetic-energy spectrum with no first-order change in the shape of the spectrum an approximate one-to-one correspondence should exist between points on the initial kinetic-energy spectrum obtained by time-of-flight measurements and the final pulse-height spectrum obtained with the surface-barrier detectors. Figure 2 shows a Cf^{252} pulse-height spectrum obtained with the surface-barrier detectors. The energy calibration also shown in Fig. 2 was obtained assuming that a one-to-one correspondence exists between equivalent points on the pulse-height distribution and the initial kinetic-energy spectrum reported by Milton and Fraser.[20] The rather good linearity indicates the decrease in the kinetic energies for all fission-fragment masses is, indeed, approximately the same. The dashed curve in Fig. 2 represents the initial kinetic-energy spectrum determined by Milton and Fraser normalized to the same area as the spectrum obtained using a surface-barrier detector. The energy calibration obtained in this manner by (1) performing a least-squares fit using 12 representative points over the entire spectrum, (2) performing the least-squares fit over just the light or heavy fragment peaks, and (3) using just the most probable values agree to within 2% for the entire energy range of interest.

For the case of the fission of Ra^{226} and U^{238} the fission-

[20] J. C. D. Milton and J. S. Fraser, Phys. Rev. **111**, 877 (1958).

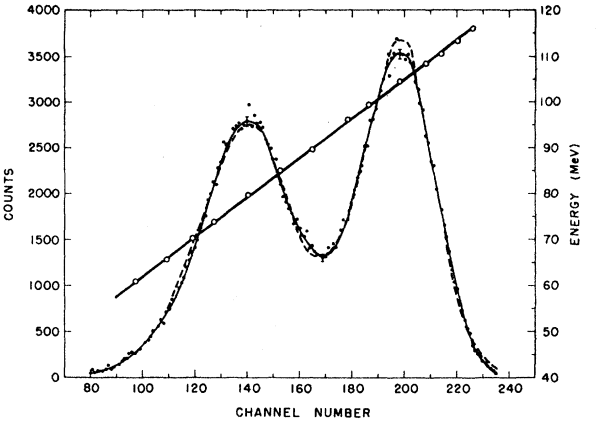

FIG. 2. Cf^{252} fission-fragment pulse-height distribution. The energy calibration shown in this figure was obtained assuming that a one-to-one correspondence exists between equivalent points on the pulse-height distribution and the initial fragment kinetic-energy spectrum reported by Milton and Fraser (Ref. 20). The initial kinetic-energy distribution of Milton and Fraser normalized to the same area as the pulse-height spectrum is shown by the dashed curve.

fragment masses and kinetic energies are very similar to those of Cf^{252} and hence the energy calibration obtained in this manner is a good approximation. The calibration for the fission of Bi^{209} requires an extrapolation of the light fragment kinetic energies and is expected to be good to 2%. There is a small error in the measured kinetic energies for these cases studied since the Cf^{252} calibration corrects to first order for the emission of only 3.8 neutrons. An estimated 5.3 and 6.7 neutrons are emitted in the fission of U^{238} with 29.7- and 42-MeV alpha particles, respectively, 4.4 and 5.4 neutrons in the fission of Ra^{226} with 31.0- and 38.7-MeV alpha particles, and 2.6 neutrons in the fission of Bi^{209} with 42-MeV alpha particles. The average number of neutrons ($\bar{\nu}$) emitted for the cases of U^{238} and Ra^{226} was estimated using the empirically determined Eq. (2) (Ref. 21)

$$\bar{\nu}=\nu_0+0.12E_e. \tag{2}$$

In this equation, ν_0 represents the number of neutrons emitted at a hypothetical zero-excitation energy and E_e represents the compound nucleus excitation energy. The number of neutrons emitted in the fission of Bi^{209} was estimated from the calculated energy available for neutron emission and the average neutron binding energies.[22] The maximum error in the reported total kinetic energies due to the different numbers of neutrons emitted in the cases studied here relative to that of Cf^{252} is less than 2 MeV. This error is smaller than the expected error due to statistical uncertainties in the energy calibration. Therefore, no further corrections

[21] J. R. Huizenga and R. Vandenbosch, in *Nuclear Reactions*, edited by P. M. Endt and P. B. Smith (North-Holland Publishing Company, Amsterdam, 1962).

[22] J. C. D. Milton, University of California Radiation Laboratory Report UCRL-9883 Rev., 1962 (unpublished).

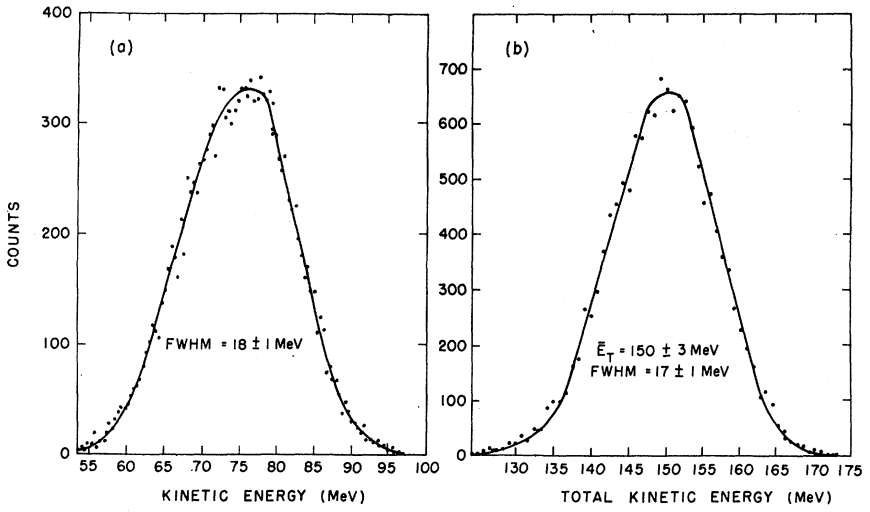

FIG. 3. Initial kinetic-energy distributions for Bi^{209} (42 MeV α,f). (a) Single fragment kinetic-energy distribution; (b) total kinetic-energy distribution.

have been applied to the reported kinetic energies for the different numbers of neutrons emitted.

III. EXPERIMENTAL RESULTS

The results of this work are based on 1.5×10^4 coincidences recorded for the bombardment of Bi^{209} and 2 to 5×10^5 events recorded for each bombardment of Ra^{226} and U^{238} with various energy alpha particles. The initial fission-fragment kinetic-energy spectra and total kinetic-energy distributions are shown in Figs. 3 through 7.

The total mass yield distributions obtained for all of the systems studied are shown in Fig. 8. The features of these initial mass yield distributions such as general shape, peak-to-valley ratio, width, etc., are qualitatively similar to the final fragment mass yield distributions obtained radiochemically.[23,24] The number of radiochemically determined mass yields for each system is small and the errors rather large. A detailed comparison of the initial and final mass yield distributions can, therefore, not be undertaken. The initial mass yield distributions

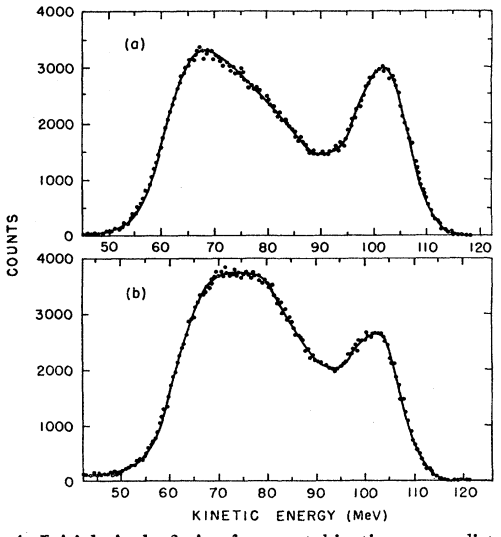

FIG. 4. Initial single fission-fragment kinetic-energy distributions for Ra^{226} (α,f). (a) $E_\alpha=30.8$ MeV. (b) $E_\alpha=38.7$ MeV.

[23] R. Vandenbosch, T. D. Thomas, S. E. Vandenbosch, R. A. Glass, and G. T. Seaborg, Phys. Rev. **111**, 1358 (1958).
[24] R. C. Jensen and A. W. Fairhall, Phys. Rev. **118**, 771 (1960).

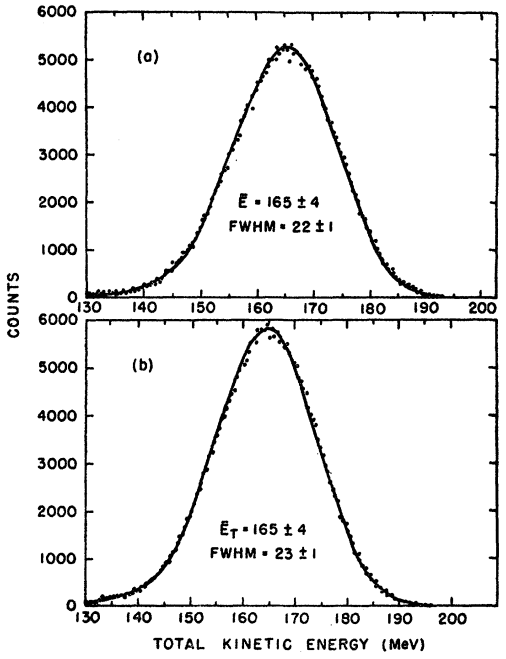

FIG. 5. Initial total kinetic-energy distributions for Ra^{226} (α,f). (a) $E_\alpha=30.8$ MeV; (b) $E_\alpha=38.7$ MeV.

for several fixed total kinetic energies are shown in Figs. 9 and 10 for the bombardments of Ra^{226} and U^{238}, respectively. These figures illustrate the strong dependence of the mass yield distributions on the total kinetic-energy release.

The dependences of the total kinetic energy and variance of the total kinetic energy on the heavy fission-fragment mass are shown in Fig. 11. In this figure the

masses associated with symmetric fission are indicated by vertical lines. As seen in Fig. 11, the maximum kinetic energies for the bombardments of Ra^{226} and U^{238} all occur at heavy fragment masses of 135 ± 1 mass units, which corresponds to masses slightly greater than the mass number of nuclei with closed 50 proton -82 neutron shells. On the other hand, the variances in the total kinetic energies are a maximum at slightly lower mass numbers of 131 ± 1.

IV. DISPERSION EFFECTS

The energy calibration used in this work corrects to first order for the average decrease in kinetic energy due to neutron emission and energy loss in the target material. However, no correction has been made for the increased dispersion in kinetic energy and hence in

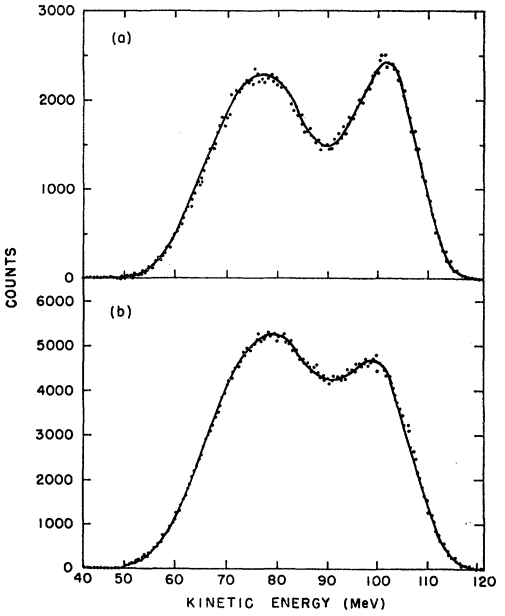

FIG. 6. Initial single fission-fragment kinetic-energy distributions for U^{238} (α,f). (a) $E_\alpha=29.4$ MeV; (b) $E_\alpha=42.0$ MeV.

the mass distribution due to these effects primarily because there is no information presently available on the details of the neutron emission at these high-excitation energies. As an example of the expected magnitude of the energy and mass dispersions due to neutron emission, we have made approximate calculations for the bombardment of U^{238} with 29.4-MeV alpha particles. The variance of the calculated heavy fragment mass, $\sigma^2(M_{HC})$, is given[15] by Eq. (3) and the variance of the measured total kinetic energy is given by Eq. (4).

$$\sigma^2(M_{HC})\cong\frac{4\bar{\nu}M_LM_Hm_n\bar{E}_n}{3A\bar{E}_K}, \tag{3}$$

$$\sigma^2(E_K)\cong\frac{2\bar{\nu}m_n\bar{E}_K\bar{E}_n}{3A}\left[\frac{M_H^2+M_L^2}{M_HM_L}\right]. \tag{4}$$

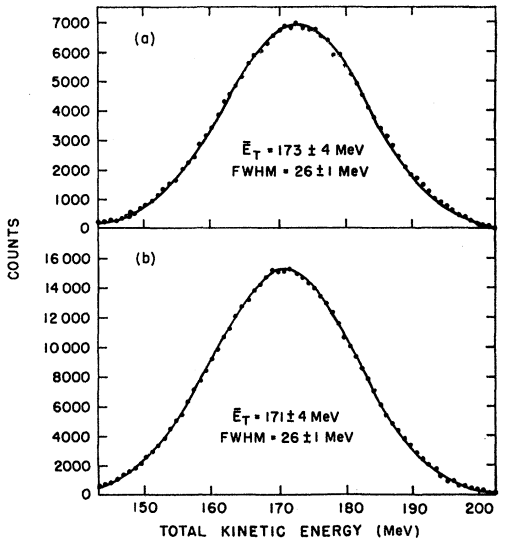

FIG. 7. Initial total kinetic-energy distributions for U^{238} (α,f). (a) $E_\alpha=29.7$ MeV; (b) $E_\alpha=42.0$ MeV.

In these equations, A, M_L, M_H, m_n represent the masses of the total fissioning nucleus, the light fragment, heavy fragment and neutron, respectively. $\bar{E}_n$ and $\bar{E}_K$ represent the average neutron energy in the center-of-mass system and the average fragment total kinetic energy. In deriving these equations the assumption is made that each fragment emits the same number of neutrons $\bar{\nu}/2$. If we consider the case of a specific fission event in

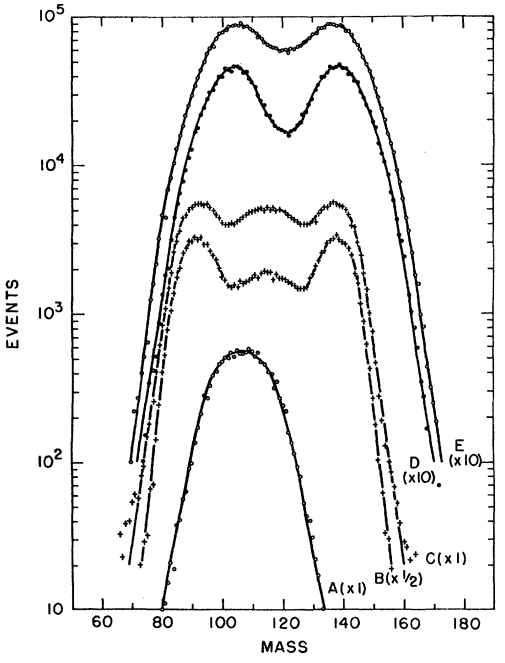

FIG. 8. Total initial mass yield distributions. For convenience of display the number of events for each system has been multiplied by a scale factor given in parenthesis. (a) Bi^{209} (42.0 MeV α,f); (b) Ra^{226} (30.8 MeV α,f); (c) Ra^{226} (38.7 MeV α,f); (d) U^{238} (29.4 MeV α,f); (e) U^{238} (42.0 MeV α,f).

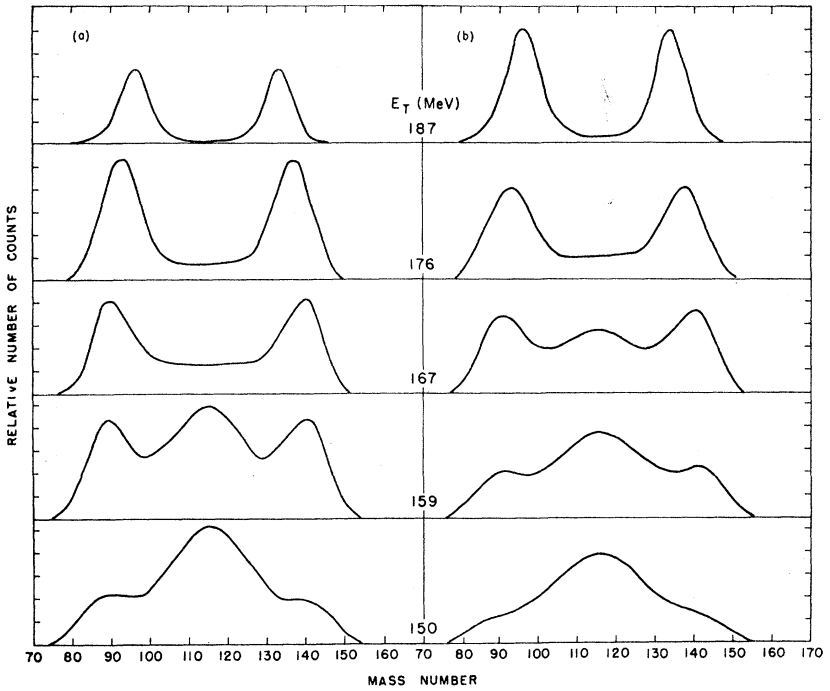

FIG. 9. Initial mass yield distributions for Ra^{226} (α,f) as a function of the total kinetic-energy release. (a) $E_\alpha=30.8$ MeV; (b) $E_\alpha=38.7$ MeV.

which fragments of masses 108 and 134 are emitted with a unique total kinetic energy of 176 MeV, the calculated heavy fragment mass would be expected to have a variance of 3.7 (mass units)^2 and the variance in the measured total kinetic energy would be 8.2 (MeV)^2. Assuming each distribution to be Gaussian, the full widths at half-height are 4.5 mass units and 6.8 MeV, respectively.

The dependences of the total kinetic energies and variances of the total kinetic energies as a function of the fission fragment masses are not appreciably affected by the expected dispersion in the calculated fragment masses due to neutron emission and the source thicknesses used in this work. The mass dispersions due to finite source thickness are due to the varying energy losses of fragments originating at different positions in

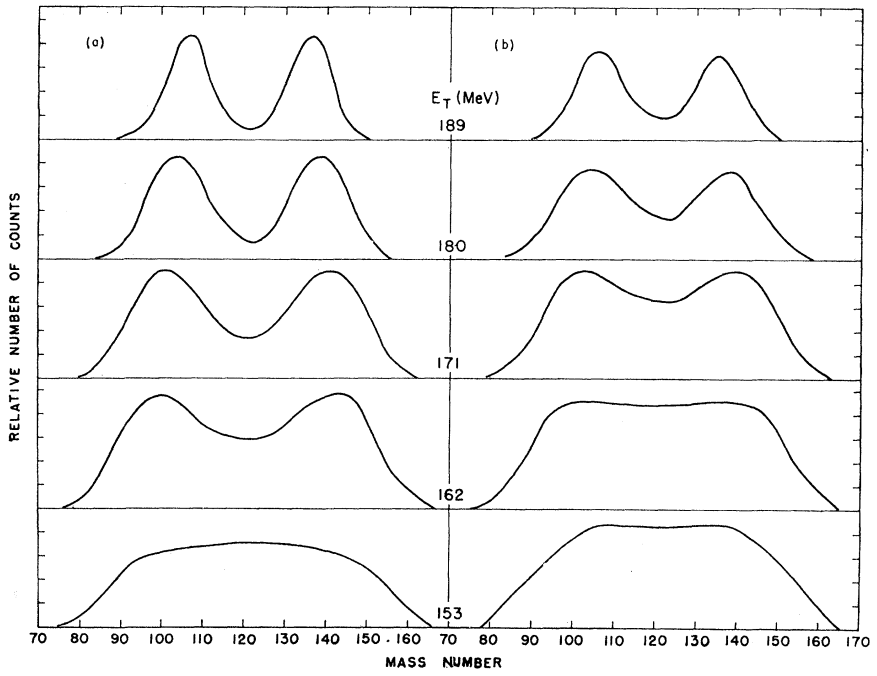

FIG. 10. Initial mass yield distributions for U^{238} (α,f) as a function of the total kinetic-energy release. (a) $E_\alpha=29.4$ MeV; (b) $E_\alpha=42.0$ MeV.

the target material. In order to estimate the effects of such dispersions we have corrected the data for the case of U^{238} bombarded with 29.4-MeV alpha particles for these two effects. This system emits more neutrons than most of the cases studied in this work and the thickest target was used in this particular study. Therefore, with the exception of U^{238} plus 42-MeV alpha particles, the effects should be maximum. The mass dispersion due to neutron emission was assumed to be Gaussian and given by Eq. (3). The dispersion due to the target thickness which is a rectangular function was then folded into the calculated mass dispersion due to neutron emission. Using this calculated total mass resolution function the resolution effects were then unfolded from the measured total kinetic energy versus fragment mass curve. The resultant corrected curve is shown in Fig. 11 as a dashed curve. The change in kinetic energy due to the mass resolution was <1 MeV for all masses to mass 155 and is not important for the following discussions presented in this paper. The increase in the variance of the kinetic energy due to the mass resolution was calculated using the same mass resolution function assuming that all fragments had the same intrinsic variance of 68 MeV^2. With this assumption the increase in the total kinetic-energy dispersion due to the mass dispersion was $\leqslant 2$ MeV^2 for all masses. The increases in the variances at mass 131 are, therefore, not artificially due to the experimental mass resolutions but are inherent in the fission process itself.

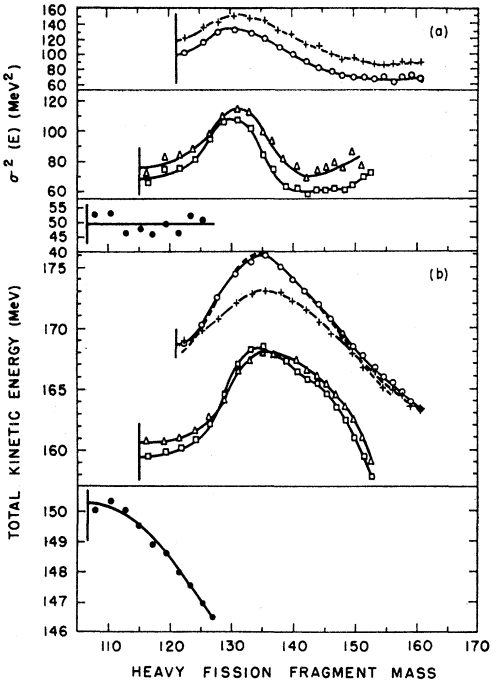

FIG. 11. Initial total kinetic-energy distributions as a function of the heavy fragment mass. (a) Variance of the total kinetic-energy release; (b) Total kinetic-energy release; ●, Bi^{209} (42 MeV α,f); □, Ra^{226} (30.8 MeV α,f); △, Ra^{226} (38.7 MeV α,f); ○, U^{238} (29.7 MeV α,f); +, U^{238} (42.0 MeV α,f). The dashed curve represents the data for U^{238} (29.7 MeV α,f) corrected for mass resolution.

V. DISCUSSION

The average total kinetic energies measured for helium-ion-induced fission of Bi^{209} (42-MeV bombarding energy), Ra^{226} (30.8 and 38.7 MeV) and U^{238} (29.4 and 42.0 MeV) are 150±3, 165±4, 165±4, 173±4, and 171±4 MeV, respectively. These values increase with $Z^2/A^{1/3}$ in a way consistent with the correlations of Terrell[25] and Viola and Sikkeland.[26] The data are also in agreement with the predictions of the model of Swiatecki and Nix[27] in which the nucleus is assumed to be a uniformly charged liquid drop with a sharp surface. In the latter model the nuclear fluid is assumed to be incompressible, nonviscous and irrotational. Within experimental error the above experimental values of the most probable total kinetic energies fit the solid curve in Fig. 3 of Ref. 27 for fragments with nonviscous irrotational flow. With the opposite assumption of infinitely viscous fragments (top curve in Fig. 3 of Ref. 27), kinetic energies are predicted which are larger by 10–15 MeV.

The experimental values of the FWHM (full width at half-maximum) in the total kinetic energy are also of theoretical interest. With the nonviscous model of Nix the calculated (to lowest order) kinetic-energy distribution is Gaussian centered about the most probable value of the kinetic energy. The FWHM is temperature-dependent and as the temperature approaches zero, the FWHM approaches a finite value determined by the quantum-mechanical zero-point vibrations. In addition it should be emphasized that the calculations of Nix are for the case where the saddle point is coincident with the scission point. More detailed liquid drop calculations[28] have shown that for $x<0.7$ this is a very good approximation. It has been shown earlier that helium-ion-induced fission of Bi^{209} leads to single chance fission,[11] and hence experimental data from this fissioning system are especially appropriate for comparison with the calculations of Nix. Subtracting a fission threshold[29] of 16 MeV for At^{213} ($x=0.677$) gives a residual excitation energy E above the saddle point of 16 MeV. From the relationship[30] $E=at^2-t$ and the empirical equation[30] $a=A/8$, the thermodynamic temperature for At^{213} at the saddle-scission configuration is 0.8 MeV. Nix has calculated for a fissioning nucleus with $x=0.677$, a FWHM of approximately 16 MeV for $t=0.8$ MeV. The uncorrected experimental FWHM for the fission

[25] J. Terrell, Phys. Rev. **113**, 527 (1959).
[26] V. E. Viola, Jr., and T. Sikkeland, Phys. Rev. **130**, 2044 (1963).
[27] W. J. Swiatecki (private communication, 1961); J. R. Nix, University of California Radiation Laboratory Report UCRL-10695, 1963 (unpublished).
[28] S. Cohen and W. J. Swiatecki, University of California Radiation Laboratory Report, UCRL-10450, 1962 (unpublished).
[29] R. Chaudhry, R. Vandenbosch, and J. R. Huizenga, Phys. Rev. **126**, 126 (1962).
[30] K. J. LeCouteur and D. W. Lang, Nucl. Phys. **13**, 32 (1959).

of At^{213} is 17 ± 1 MeV. As discussed in Sec. IV, the experimentally observed FWHM has to be corrected for dispersion introduced by neutron emission and experimental conditions. Correcting for these dispersion effects gives a FWHM of 16 ± 1 MeV in excellent agreement with the above calculations.[31] The magnitude of the FWHM develops from an "amplification process" in which very small uncertainties in the potential energy give large differences in the kinetic energy.[27,32]

As already indicated no theory exists at this time for computing theoretical values of the FWHM in the total kinetic energy for helium-ion-induced fission of U^{238} and Ra^{226}. These fissioning plutonium isotopes ($x=0.728$ to 0.738) have cylindrical saddle configurations[28] and the fissioning thorium isotopes ($x=0.703$ to 0.712) have more stretched out saddle points, however, the two spheroid saddle configuration is probably still a poor approximation. In addition these fissioning nuclei show structure in their kinetic energies as a function of fission product mass, a result not predicted by the simple liquid drop theory.

The mean kinetic energies (see Figs. 5 and 7 for values) observed in the fission of U^{238} and Ra^{226} with energetic helium ions are within experimental error equal to the values of 175 ± 2 and 160 ± 3 observed by Milton and Fraser[33] and Smith *et al.*,[34] respectively, for comparable fissioning systems formed by thermal capture on Pu^{239} and Th^{229}. This close agreement in mean kinetic energies for like fissioning systems with greatly different excitation energies substantiate earlier findings that little if any of the bombarding energy of the projectile is converted into kinetic energy of the fragments. However, the good agreement in mean kinetic energies for different excitation energies is somewhat fortuitous since the dependence of total kinetic energy on fission fragment mass observed in these experiments is quite different from that observed for thermal-neutron-induced fission (compare the data in Fig. 11 for $U^{238}+He^4$ fission with the data in Fig. 8 of Ref. 3) for $Pu^{239}+$thermal neutron fission). The thermal neutron data give a larger peak kinetic energy (at about the same fission-fragment mass) which falls substantially faster as the fission-fragment mass is either increased or decreased. The similar average kinetic-energy values for different type and energy fission arise from dissimilar kinetic energy versus mass distributions weighted with dissimilar mass yield curves. To first order these kinetic energy and mass distributions for different excitation energies appear to compensate each other to give a constant kinetic energy.

The mass yield curves displayed in Fig. 8 show the markedly different distributions for helium-ion-induced fission of Bi^{209}, Ra^{226}, and U^{238}. Fission of Bi^{209} with alphas gives the typically observed single-humped mass yield curve observed for low Z elements. On the other hand, fission of U^{238} with alphas gives a two-humped mass yield distribution with the valley between the peaks becoming shallower with increasing excitation energy. Helium-ion-induced fission of Ra^{226} gives a three-humped mass yield distribution. The peak intensity of the heavy fragment in the fission of Ra^{226} and U^{238} comes at a mass of approximately 138, although for the highest bombarding energy of U^{238} the peak has shifted slightly toward a lower mass. The placement of the heavy mass peak appears to be a rather general feature of heavy-element fission independent of excitation energy.

The dependence of the total kinetic energy as a function of fission product mass for the various fissioning systems are shown in Fig. 11. The structure in the total kinetic energy versus mass curves for Ra^{226} and U^{238} is thought to be associated with nuclear structure. From the various experimental and theoretical investigations, the following model for fission is emerging. The scission configuration is a function of the fragment masses of which it is composed and varies markedly for different pairs of fragments. If the nuclear structure is such that the potential energy of the system is minimized by an unusually large deformation at the scission point, the Coulomb interaction energy between the fragments is smaller than average, and such a configuration leads to a reduced value of the final total kinetic energy (the interaction energy is dissipated largely in the form of kinetic energy of the final fragments). While mass splits associated with these large deformations at the scission point give reduced values of the kinetic energy, the primary fission fragments are predicted to have large excitation energies and to emit an unusually large number of prompt neutrons. Evidence exists that thermal-neutron-induced fission gives an enhanced number of neutrons for symmetric mass splits where the kinetic energy is low.[17–19] However, the kinetic-energy data of Fig. 11 give a scission shape less deformed than that for thermal-neutron fission at mass symmetry which is consistent with the expectation of a much smaller enhancement of neutron yield at symmetry.

The maximum in the total kinetic energy for Ra^{226} and U^{238} at $M_H=135\pm1$ is interpreted in terms of a reduced effective separation distance at the scission point resulting from the stiffness to distortion of the doubly closed-shell core of the heavy fragment. Such a configuration would give a lower excitation energy for the fragment near shells (fewer prompt neutrons) and a larger excitation energy for the complementary fragment (more prompt neutrons). Thermal-neutron fission experiments have shown a correlation between nuclear shells and number of prompt neutrons in fission. However, the detailed division of internal energy at the scission point is not understood at this time. Compa-

[31] The FWHM experimental data shown in Fig. 6 of Ref. 27 have been over-corrected by that author for the dispersion effects due to neutron emission from the fragments.
[32] R. Vandenbosch, Nucl. Phys. (to be published).
[33] J. C. D. Milton and J. S. Fraser, Can. J. Phys. **40**, 1626 (1962).
[34] A. Smith, P. Fields, A. Friedman, and R. Sjoblom, Phys. Rev. **111**, 1633 (1958).

rable neutron energies have been observed from fragments which emit very different numbers of neutrons.[17] The reduction in kinetic energy for other mass splits (i.e., beyond the expected reduction in kinetic energy due to the unequal charges of the two fragments) is assumed on this model to be associated with a greater separation of the effective charges at the point of minimum potential energy or scission configuration.

It is of interest to compare in more detail the kinetic-energy distributions observed in this work with comparable fissioning nuclei excited with thermal neutrons. The observed maximum value of the kinetic energy at 135 ± 1 mass units is about 2 mass units larger than the mass at which the maximum kinetic energy is observed for thermal-neutron fission of Pu^{239}. In addition, the shapes of the kinetic-energy distributions for Ra^{226} and U^{238} shown in Fig. 11 are quite different from those observed in thermal neutron fission of Pu^{239} and Th^{229} (Refs. 33 and 34, respectively). The kinetic energies for masses below and above the mass of maximum kinetic energy are considerably larger for fission induced with higher excitation energy. For example, the average total kinetic energy decreases in going from mass 135 to symmetry and from mass 135 to 150 by factors of 4 and 2, respectively, times as much for thermal neutron fission of Pu^{239} as observed for fission of U^{238} with alpha particles. The higher excitation energy has raised not only the total kinetic energy at symmetry but also for mass splits giving large values of the heavy fragment masses. For these heavy fragment mass values the implied smaller effective separation of charge centers in the case of high-energy fission may be due to changes in the viscosity and tensile strength of the nuclear fluid with increased temperature. The nuclear viscosity is expected to increase with excitation energy giving rise to a slight increase in the kinetic energy of a particular pair of fragments. For infinitely viscous fragments, the kinetic energy is predicted[27] to approach the Coulombic interaction energy of the scission configuration. The tensile strength of nuclear matter is expected to decrease with increasing excitation energy. The large distortions in the fragments at the scission configuration will be less likely since the nuclear matter would tend to break apart earlier. These effects tend to increase the fragment kinetic energies for higher bombarding energies in mass regions where for low-energy fission the fragments were very cold at the scission configuration. Halpern[35] has discussed nuclear viscosity and tensile strength in enumerating factors which may influence charged-particle emission in fission.

The mass yield curves of helium-ion-induced fission of Ra^{226} and U^{238} for fixed values of the total kinetic energy as displayed in Figs. 9 and 10 can be understood in terms of the relationship between the kinetic energy and fission-fragment mass plotted in Fig. 11. The mass yield curves for the highest total kinetic energies are asymmetric with the heavy mass peak at approximately 135 mass units. For smaller values of the total kinetic energy the heavy peak mass is double valued (see Fig. 11) and hence the mass yield curve becomes more complex with a filling in of the region near symmetric fission. For Ra^{226} fission, total kinetic energies near 160 MeV give a triple-humped mass yield curve with the three peaks having approximately equal intensities.

In Fig. 11 the variance in total kinetic energy is plotted as a function of the heavy fission product mass for helium-ion-induced fission of Bi^{209}, Ra^{226}, and U^{238}. The ordinate parameter σ^2 (variance) is related to the FWHM by FWHM (MeV) $=2.354\,\sigma$ (MeV). The plotted variances have not been corrected for dispersion effects introduced by neutron emission and experimental conditions. However, as discussed in Sec. IV, these effects make only a very small reduction in the plotted variances. The variance for Bi^{209} fission is essentially independent of heavy fission-fragment mass while the variances for Ra^{226} and U^{238} fission each have a maximum at $M_H=131$. These two fissioning targets with masses differing by 14 mass units give a maximum variance at two different bombarding energies at the same value of M_H. The larger variance for $M_H=131$, therefore, appears to be associated with a particular type of fission mode which is influenced by the nuclear structure of M_H rather than M_L. In terms of a model in which the variance depends on the "amplification factor" mentioned earlier, mass splits with $M_H=131$ may have a scission configuration with a broad shallow potential energy minimum as a function of distortion. Although the mass dependence of the variance in the total kinetic energy can be qualitatively explained by the so called "two mode fission hypothesis,"[8] the maximum variance at $M=131$ must ultimately be related to nuclear structure and result from a "many-mode fission process."

The position of maximum variance in the average total kinetic energy is shifted downward by about 4 mass units from the maximum in the average total kinetic energy. This implies that the dispersion at $M_H=131$ is slightly greater than for mass splits with $M_H=135$. The dependence of the variance on M_H for helium-ion-induced fission of U^{238} is considerably different from the variance observed for thermal neutron fission of Pu^{239} (see Fig. 13 of Ref. 33). Although the details of the differences are not understood at this time. the markedly different nuclear temperatures at the scission configuration in the two different experiments probably plays an important role.

ACKNOWLEDGMENTS

We gratefully acknowledge the aid of Dr. George L. Bate during the early part of this work and Dr. J. E. Gindler for preparation of the radium targets.

[35] I. Halpern (private communication, 1963).